Chapter 6

Convective-scale Modelling

Authors: Stuart Webster[1], Steven Chan[2], Muhammad Eeqmal Hassim[3], Elizabeth Kendon[1], Charline Marzin[1], Sandeep Sahany[3] and Claire Scannell[1].

Met Office internal reviewers: Simon Vosper[1], Gill Martin[1] and Julia Slingo[1]

1 - Met Office, Exeter, UK

2 - Newcastle University, Newcastle, UK

3 - Centre for Climate Research Singapore, Singapore

Contents

6.1 Introduction

The aim of this study (referred to as Stage 3b) is to simulate the climate of Singapore using a high-resolution convection-permitting RCM, and compare these simulations with those using the lower-resolution parametrized-convection RCM used in Chapters 4 and 5 of this project (referred to as Stage 3).

As highlighted by Kendon et al. (2012), there are a number of potential advantages from using a convection permitting RCM. In particular some of the well-known weaknesses associated with RCMs which employ a convection parametrization, such as the maximum in rainfall over land occurring too early in the day and the lack of realistic variability on sub-daily timescales, are likely to be improved. Furthermore, improving the realism of the rainfall on these sub-daily timescales implies there is improved skill in modelling the underlying physical processes. With this foundation, it is possible that the convection permitting RCM might also improve aspects of the simulated climate on longer timescales, e.g. the timing of the seasonal cycle or the duration of dry spells.

The major disadvantage of using a convection permitting RCM is the computational cost. The RCM domain needs to be of sufficient size that the central area of the domain is (at worst) only weakly affected by the lateral boundary conditions provided by the driving model. The mesh-size used in convection-permitting models is typically 1 km to 5 km, and hence the minimum horizontal mesh for credible climate simulations is of the order of a couple of hundred grid-points in each direction. The relatively large number of grid-points, together with the relatively short timestep which must be used in these models, mean that multi-year convection permitting RCM simulations have only recently been attempted. Indeed, the only convection permitting RCM study using the Met Office Unified Model is for a southern UK domain (Kendon et al. (2012), Kendon et al. (2014)).

In this study a convection permitting RCM is used for the first time (as far as we are aware) to simulate the climate for a region in the deep tropics. The convection permitting RCM used is the one developed within the SINGV Numerical Weather Prediction (NWP) project, and is based on the very latest “state-of-the-art” version of the UK area 1.5 km model known as the UKV. The work undertaken is therefore highly experimental, since there is no previous experience to build on with regard to using a convective-scale RCM in the tropics and hence the model has not been optimised in any way for climate rather than NWP applications.

The simulations are centred on Singapore with a 1.5 km RCM nested inside the 12 km RCM. In order to maximise in an affordable way the area over which the convective-scale modelling approach is employed, an intermediate 4.5 km convection permitting RCM is also employed. In this way there is at least 800 km of explicit convection simulation between Singapore and the parametrized-convection 12 km RCM driving simulation.

The main aim of this study is to improve the understanding of daily and sub-daily rainfall variability which is known to be deficient in 12 km RCM simulations. The impacts on the mean climate are also investigated and, finally, the assumptions that have been made in the bias correction of rainfall over Singapore in Chapter 5 are assessed.

The outline of the remainder of this report is as follows. Section 6.2 provides details of the model configuration, whereby a 1.5 km convection permitting model is nested inside the 12 km RCM (with minor modifications) used in Chapters 4 and 5. Section 6.3 describes the results, first considering the simulation of the present day climate and then assessing the projected climate change signals. Results summarised in Section 6.4 and finally in Section 6.5 recommendations and limitations of this study are discussed.

Note that throughout this document some summary plots and examples of individual model results are shown. Supplementary plots are included in an Appendix to this chapter and referred to in the text with figure numbers prefixed with the reference 'A'.

6.2 Methodology

In this section, the details of the nesting procedure used to perform the convective-scale simulations are described. Figure 6.1 (a) shows the areal extent of the three limited area model domains used. The highest resolution model, outlined in black, is a 1.5 km RCM, which uses a domain of 390×390 grid points, centred on Singapore. As Figure 6.1(b) shows, 1.5 km resolution is sufficient to resolve many of the small islands in the Malacca Strait and, indeed, at this resolution Singapore itself is almost completely detached from Malaysia because the Johor Strait is resolved (this feature is more clearly seen in Figure 6.11).

The 1.5 km RCM is one-way nested inside a second convective-scale model which has a resolution of 4.5 km and which also uses a domain of 390×390 grid points. The extent of the 4.5 km RCM is shown by the solid white line in Figure 6.1(a) which also indicates that it is centred slightly to the west of Singapore. This offset to the west ensures that Sumatra, and its associated mountain chain lie within the 4.5 km domain and hence ensures that Sumatran squall rain events can be explicitly represented in this pair of convective-scale models. Finally the 4.5 km RCM is nested inside a 12 km RCM which is essentially the same as used for the main downscaled projections, but has been extended to the west (and slightly to the south) to ensure an adequate 12 km resolution zone between the global driving model and the 4.5 km RCM. The only other difference between the 12 km RCM used here to that documented in Supplementary Information Report 1 is that the surface vegetation is derived from the International Geosphere-Biosphere Programme (IGBP) 1 km resolution dataset to ensure consistency with the 4.5 km and 1.5 km RCMs which also use this dataset.

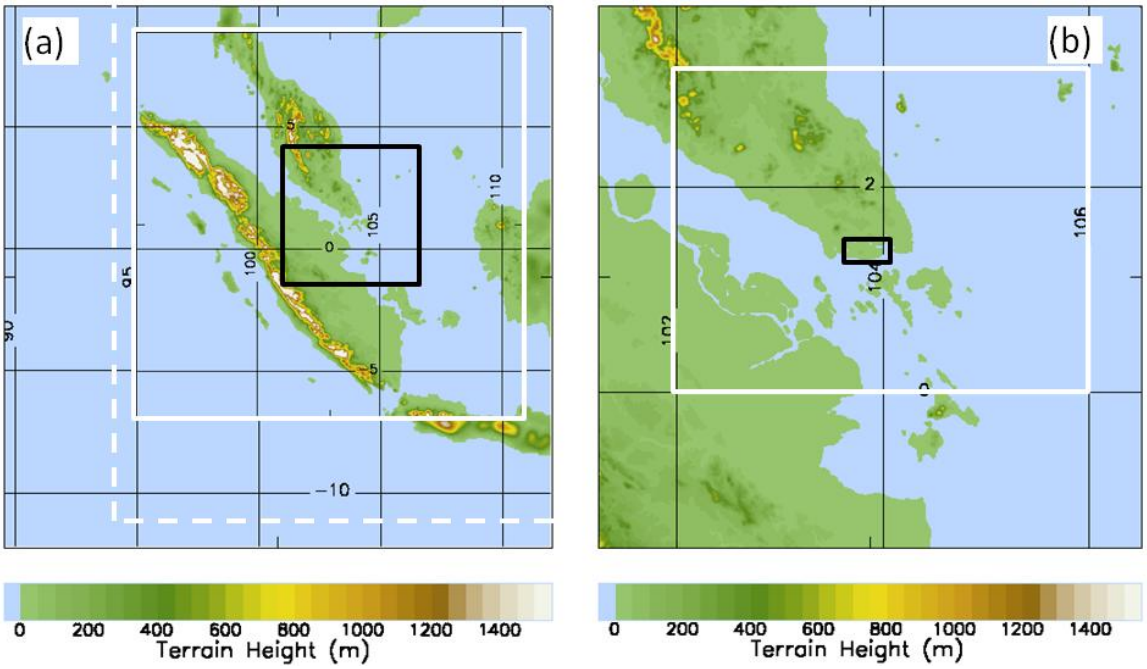

Figure 6.1: The model domains, land-sea mask and orography used in this study. (a) The full area shows the south-west corner of the 12 km domain. The dashed white line shows the southern and western limits of the 12 km domain used for Chapters 4 and 5. The solid white line denotes the limits of the 4.5 km domain whilst the solid black line shows the limits of the 1.5 km domain. (b) A zoom of the 1.5 km domain, with the solid white line showing the area over which most of the subsequent analysis has been performed, and the solid black line showing the area over which the data was averaged to produce the timeseries shown in Figure 6.3.

The configuration used for the convective-scale models is the "version 1" configuration which has been developed and tested over the last fifteen months as part of the SINGV project. This configuration is similar to that used in Kendon et al. (2012), but with a number of enhancements, which are described, together with other technical details, in the Appendix to Chapter 6.

Three simulations each of 10 years duration have been performed using this nesting procedure. In the first, the 12 km RCM was driven by ERA-interim analyses from June 2000 to June 2010. The other two simulations were both driven by HadGEM2-ES with one present day simulation (June 1995 to June 2005) and one RCP8.5 simulation (June 2089 to June 2099). The 10 year periods were chosen so that the mean El Nino signal over the simulation period was as close to neutral as possible with the aim of minimising the contamination by El Nino on any climate change signal in these relatively short climate simulations.

Although the length of these simulations is relatively short in climate modelling terms, one issue encountered when running at 1.5 km resolution and hence using a 50 second timestep, was that the throughput of the simulations was at best three months per day. Therefore, in order to complete the simulations in a timely manner, both the 4.5 km and 1.5 km simulations were split into sub-ten-year time slices. Each 10 year simulation period is therefore made up of between three and six timeslices with, in each case, the simulations overlapping by three months so that this period can be discarded as spin-up for the later simulation. Figure S1.2 of the Supplementary Information Report 1 on 12km Dynamical Downscaling indicates that a three months spin-up period will reduce significantly the discontinuity in the flow fields within the simulations. In particular, the

near-surface soil moisture field which can take some time to adjust has been shown to be approximately two-thirds of the way towards being fully spun up after this time. Obviously, it would have been preferable to have the soil moisture field fully spun up when the simulations were joined together. However, the additional computational cost of extending the spin-up period meant that this was not possible.

Finally, it is worth emphasising that the sixty years of convective-scale simulations completed successfully without a single numerical failure. The robustness of this configuration is we believe a result of using the ENDGame dynamical core, and also the accumulation of improvements from testing this configuration in the SINGV project.

6.3 Results

In this section the key results from the three simulation periods are presented. The analysis focuses on the performance of the 1.5 km RCM relative to the 12 km RCM; only a brief analysis of the performance of the intermediate 4.5 km RCM is presented here with a detailed analysis left as a subject for future work. Furthermore, the analysis focuses on the November to January (NDJ) period which is the wettest season of the year.

Section 3.1 focuses on the simulations driven by ERA-interim and hence evaluates the ability of the two models to simulate realistically the present-day climate. The mean state is assessed both on seasonal and daily timescales whilst the variability is assessed by investigating the ability of the models to capture daily and sub-daily extremes. Section 3.2 focuses on the HadGEM2-ES driven simulations in order to assess the consistency of the climate change projections deduced from the two versions of the RCM. Again, the mean climate and extremes are assessed and, in addition, an analysis of the projected change in rainfall intensity and duration is made. Finally, section 3.3 uses the results presented in section 3.2 to evaluate the assumptions that have been made in the bias correction of rainfall over Singapore in Chapter 5.

6.3.1 Present-day evaluation

6.3.1.1 Mean Climate

In this section the ERA-interim driven simulations are compared with each other and against the Tropical Rainfall Measurement Mission (TRMM) rainfall dataset in order to assess the impact of the 1.5 km RCM on the known biases of the 12 km RCM. These biases are evident in Figures 6.2(a) and (c) which show the 12km RCM NDJ mean rainfall and bias relative to TRMM. The heaviest rainfall occurs over the sea, where it is generally wetter than TRMM observations, whilst it is driest over the Malaysian Peninsula, both in an absolute sense and also relative to TRMM observations.

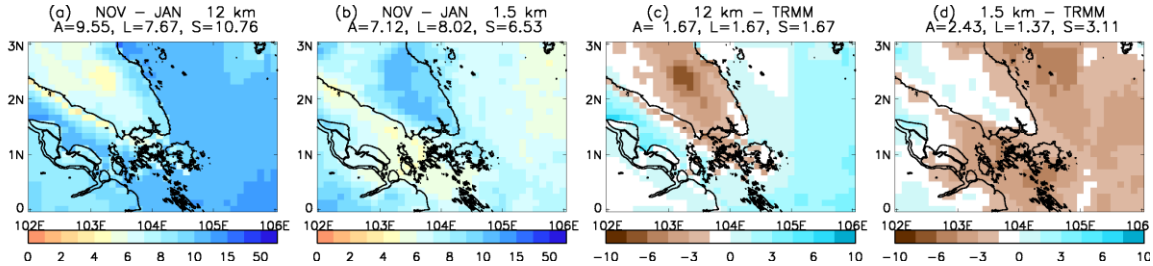

Figure 6.2: The November to January mean rainfall in mm d^{-1} for (a) the 12 km RCM, (b) the 1.5 km RCM, (c) the 12 km RCM minus TRMM and (d) the 1.5 km RCM minus TRMM. In the title of each plot the means (for (a) and (b)) and root-mean-square differences (for (c) and (d)) are shown for all points (A), land points only (L) and sea-points only (S). Note that the 1.5 km RCM data was coarse-grained onto the 12 km RCM grid and the 12 km RCM land/sea mask was used when calculating the domain averages and root mean square differences.

Figure 6.2(b) shows that the mean rainfall distribution for the 1.5 km RCM is very different to that in the 12 km RCM; the rainfall over the sea is greatly reduced whilst, where the rainfall over the Malaysian Peninsula is a domain minimum in the 12 km RCM, it is a domain maximum in the 1.5 km RCM. The 1.5 km RCM rainfall distribution therefore appears to counter the 12 km RCM rainfall biases. Figure 6.2(d) confirms that this is indeed the case over the Malaysian Peninsula, with the large dry bias reduced to close to zero. However, over the sea, the 12 km RCM wet bias has been replaced by a dry bias of comparable amplitude. Moreover, the domain averaged rainfall shown in the titles of Figures 6.2(a) and (b) indicates that the 1.5 km RCM is approximately 25% drier than the 12 km RCM (and 20% drier than TRMM, not shown). For Singapore itself, the rainfall bias is almost the same in both models.

Figure A6.1 shows the rainfall distribution for the other three seasons. The leftmost two columns indicate that the differences between the two RCMs noted above, namely that the 1.5 km RCM is wetter over land and drier over the sea, persist throughout the year. Furthermore, the 1.5 km RCM remains drier than both the 12 km RCM and TRMM throughout the year. The rightmost two columns show that these differences equate to the 1.5 km RCM having a wet bias over land and a dry bias over the sea for these three seasons.

For the 12 km RCM the bias over land is also generally positive, but smaller, whilst the bias over the sea is smaller than for the 1.5 km RCM. The net effect of these seasonal biases over Malaysia (too dry in NDJ and too wet in the other three seasons) is that the 12 km RCM annual mean rainfall bias (not shown) is close to zero. This small annual mean bias, if considered in isolation, is clearly misleading and hence we have chosen to focus on the (observed and modelled) wettest season, rather than simply present annual mean results.

In order to better understand the origin of the differences between the 1.5 km RCM and the 12 km RCM, the performance of the two models relative to the intermediate 4.5 km RCM is now investigated. In the appendix to Chapter 6, Figure A6.2 shows the seasonal mean rainfall differences between the 1.5 km RCM and the 4.5 km RCM (Figures A6.2(a)-(d)). A comparison of these difference plots with the 1.5 km RCM biases relative to TRMM (Figure 6.2(d) and the rightmost column of Figure A6.2, which are all shown on the same scale) shows that the 1.5 km RCM minus 4.5 km RCM differences are much smaller than the 1.5 km RCM biases relative to TRMM. In other words, the simulated rainfall in the 1.5 km and 4.5 km convection permitting models is very similar, and hence

the differences between the 1.5 km RCM and the 12 km RCM must be due to differences between the 4.5 km RCM and the 12 km RCM.

The differences between the 4.5 km RCM and the 12 km RCM are shown in Figures A6.2(e)-(h). Note that the region shown spans the entire 4.5 km domain, including its rim region. As deduced above, these differences are indeed much larger than the 1.5 km minus 4.5 km differences (Figures. A6.2(a)-(d)), both over the region spanned by the 1.5 km RCM (the inner part of Figures A6.2(e)-(h)), and over the full 4.5 km domain. The differences between the 1.5 km and the 12 km RCM identified above are equally as evident over this larger area, with increased rainfall over land and reduced rainfall over the sea. In particular, the 1.5 km RCM dry bias over the sea in NDJ (Figure 6.2(b)) is seen to extend all the way to the northern boundary of the 4.5 km RCM (Figure A6.2(e)). In addition, there are some large differences which appear to be associated with the adjustment of the 4.5 km RCM to the drier lateral boundary conditions supplied by the 12 km RCM (the drier 12km RCM explains why the entire rim region of the 4.5 km RCM is drier in all four seasons). Some of these differences extend significant distances into the domain, e.g. the dry bias in NDJ along the western boundary extends approximately 250 km into the domain (Figure A6.2(e)). The significant distances that these differences extend into the domain suggest that the 4.5 km simulation, and by implication the 1.5 km simulation, could be sensitive to the size of the 4.5 km RCM domain.

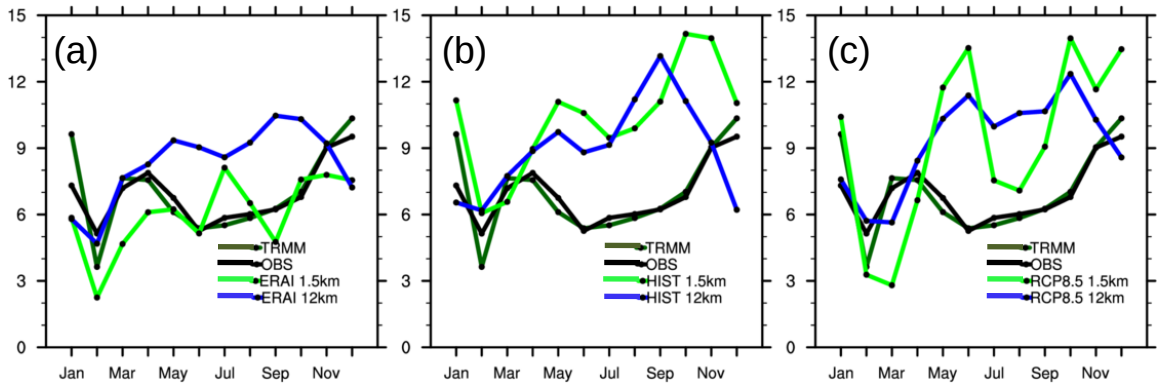

Figure 6.3: The monthly mean rainfall (in mm day^{-1}) over Singapore. On each panel are shown observations derived from TRMM and from averaging over the Singapore rain gauge network (the 28 stations shown in Figure 6.11) together with one driving model pair of model simulations. (a)The ERA-interim driven simulations. (b) The HadGEM2-ES present day simulations. (c) The HadGEM2-ES RCP8.5 driven simulations.

Returning now to the direct comparison of the 1.5 km and 12 km RCMs, an alternative way of viewing the mean climate over Singapore is shown in Figure 6.3 in which the annual cycle of monthly mean rainfall is presented. For the ERA-interim driven simulations (Figure 6.3(a)) the peak rainfall in the 12 km RCM occurs in September, three months earlier than in observations. The bias in the timing of the peak rainfall is significantly improved in the 1.5 km RCM, with the peak (associated with the north east monsoon) shifted to November.

Figure 6.3(a) also confirms that the dry bias of the 1.5 km RCM persists throughout the year. The exception to this is July, which is both significantly wetter than observations and is also the wettest month of the year for the 1.5 km RCM. A possible reason for the excessive July rainfall can be proposed following an inspection of Figures A6.1(f) and (h) which show the 1.5 km model rainfall distribution and bias relative to TRMM for June to August (JJA). The plots show that the heaviest and most excessive rainfall is confined to

the western half of the domain that includes the sea in the Malacca Strait. At this time of year the southwest monsoon prevails and Sumatran Squalls, which approach Singapore from the west, are common. These diagnostics therefore suggest that it is possible that the simulation of these events in the 1.5 km RCM is producing too much rainfall, whether that is through increased intensity, increased duration or increased frequency. However, the reasons behind this excessive rainfall in July (and to a lesser degree in August) have not been investigated and so it is proposed that such an investigation be a topic of future work.

6.3.1.2 Diurnal Cycle

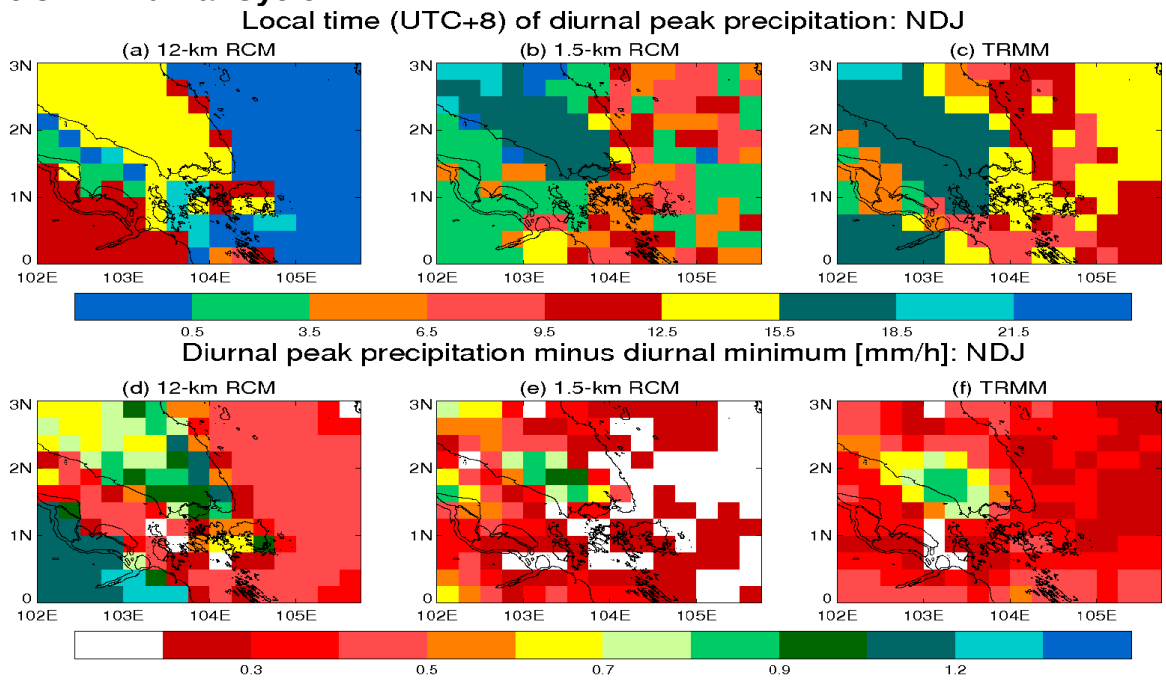

Figure 6.4: The local time of the diurnal peak precipitation (top row) and the amplitude of the diurnal cycle (bottom row) for the November to January period. (a) and (d) show the time of the peak and the amplitude of the diurnal cycle for the 12 km ERA-interim driven RCM. (b) and (e), as (a) and (d), but for the 1.5 km ERA-interim driven RCM. (c) and (f) as (a) and (d), but for TRMM. Note that the data for both the RCMs has been coarse-grained to the TRMM grid.

In this section the mean behaviour of the models is assessed on the daily timescale. Figure 6.4 shows the peak time and amplitude of the diurnal cycle for the two models and compares them to TRMM for NDJ, whilst Figure 6.5 shows the same fields for JJA.

The 1.5km RCM shows a better representation of the diurnal cycle of rainfall, both in terms of the timing of the daily maximum and the diurnal cycle amplitude. The diurnal cycle peaks too early in the 12km RCM in both NDJ and JJA - a common problem in convection-parameterised models - but TRMM may also peak too late (as suggested by CMORPH observations; not shown) and so the timing error in the 12km RCM may be slightly overestimated. The diurnal cycle amplitude is too large in the 12km RCM, which

is probably a reflection of the parameterized convection being triggered in the hours before local noon, and usually being inactive at night-time. This error is reduced in the 1.5km RCM, which is also able to capture the position of the largest diurnal variation over the Malaysian Peninsula. Both RCMs show little change in the daily timing of convection in future (not shown), but the amplitude of the diurnal cycle over land is larger, consistent with an increase in heavy rainfall.

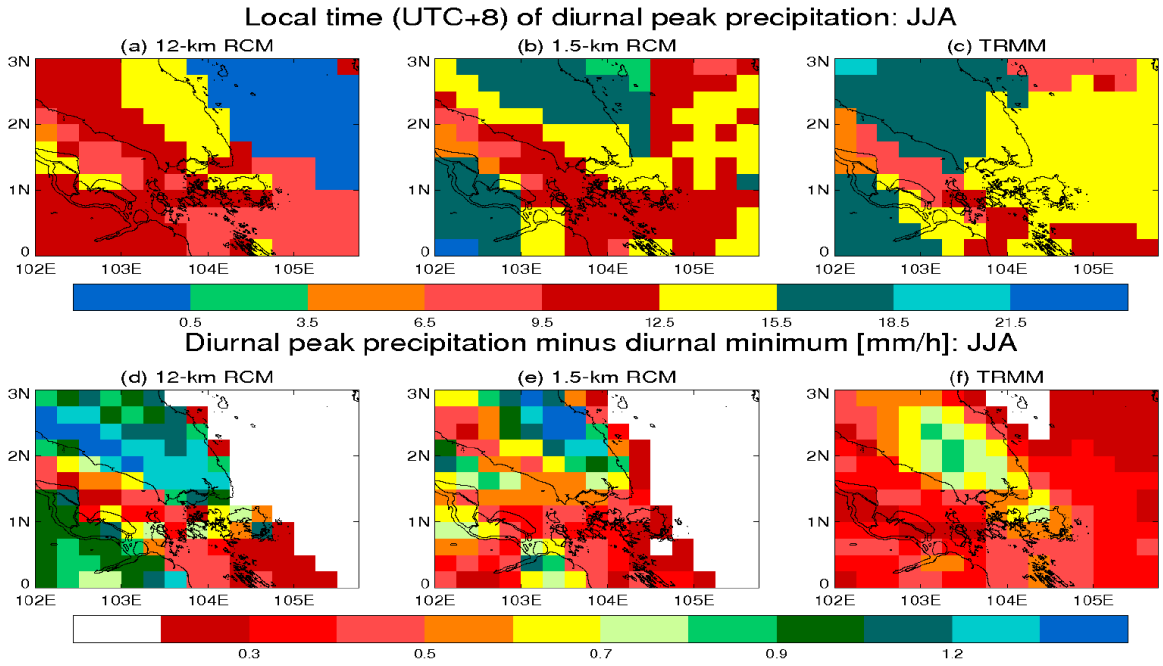

Figure 6.5: As Figure 6.4, but for the June to August period.

6.3.1.3 Extremes

In this subsection the analysis turns to the variability of the simulated climate and, in particular, the ability of the models to simulate extreme rainfall events. Figure 6.6 shows the 95th percentile of the daily rainfall totals for TRMM and for the two RCMs. The 12 km RCM significantly underestimates heavy rainfall over land in NDJ (Figure 6.6(b)), with an unrealistic sharp land-sea contrast. By comparison the 1.5 km RCM (Figure 6.6(c)) gives a much better agreement with TRMM observations (Figure 6.6(a)), and is able to capture the highest values over the coastal areas of the Malaysian Peninsula.

For the three-hourly timescale (not shown) the results are very similar to those for daily rainfall with the 12 km RCM again showing an underestimation in heavy rainfall compared to TRMM whilst the 1.5 km RCM gives much better agreement with a slight overestimation over land. However, it should be noted that compared to CMORPH observations, TRMM consistently gives higher rainfall estimates and so the dry bias in the 12km RCM may not be so severe.

In JJA the 12km RCM (Figure 6.6(e)) is too dry over both land and sea compared to TRMM (Figure 6.6(d)), with not such a sharp contrast between land and sea. In this season the 1.5km RCM (Figure 6.6(f)) is too wet over land and also has large wet biases along the Strait of Malacca. Biases in Sept-Oct are similar to those in JJA (not shown).

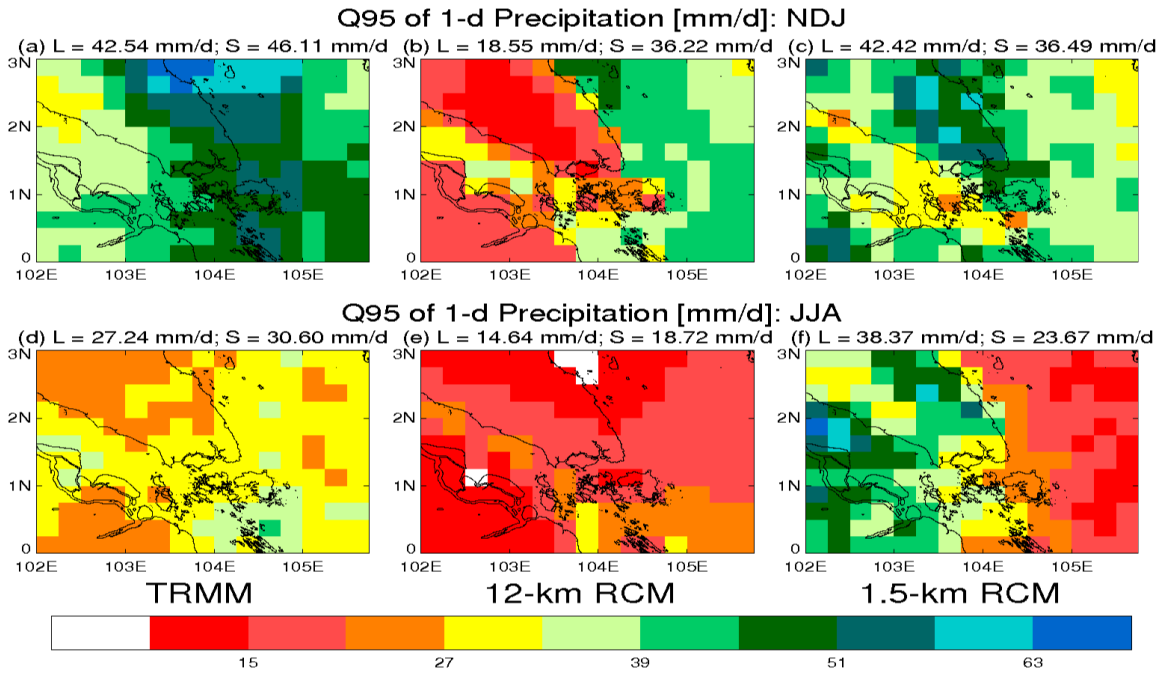

Figure 6.6: The 95th percentile of the daily precipitation totals for November to January (top row) and for June to August (bottom row). The left column shows the TRMM distribution, the middle column shows the 12 km RCM distribution and the right column shows the 1.5 km RCM distribution. Units are mm day^{-1}.

6.3.2 Climate Change Projections.

6.3.2.1 Mean Climate

In this section the horizontal resolution sensitivity of the projected climate change for mean rainfall is assessed using HadGEM2-ES as the driving model. Both 12 km and 1.5 km RCMs have been used to simulate the future climate under the RCP8.5 emissions scenario, and these simulations are compared with the present-day (also known as historical) simulations. In addition, the 12 km RCM is compared to its Chapters 4 and 5 equivalent in order to assess the robustness of its climate change signal. This is because the simulations performed in this stage of the project are relatively short (10 years long) and hence mean differences may include a significant natural variability component.

Figure 6.7 shows the NDJ seasonal mean rainfall from these simulations. By comparing the present day simulations (Figures 6.7(a) and (d)) with the ERA-interim driven simulations (Figures 6.2(a) and (b)) it is evident that there is sensitivity to the driving model and the accompanying change in SSTs. Both RCMs are much wetter when driven by HadGEM2-ES. Most strikingly, the rainfall over the sea in the 12 km RCM almost doubles when moving to the HadGEM2-ES driving model. As Figures 6.7(b) and (e) show, these changes result in smaller biases (when compared to TRMM) for the 1.5 km RCM relative to the 12 km RCM. The HadGEM2-ES SSTs, which for the domain shown are on average 1ºK warmer than the Reynolds SSTs used in the ERA-interim simulations (not shown), are almost certainly the dominant driver of these rainfall changes. The smaller biases for the 1.5 km RCM relative to the 12 km RCM in the

HadGEM2-ES driven simulations therefore appear to be due to the compensation between the 1.5 km RCM dry bias (seen in the ERA-interim simulation) and the HadGEM2-ES SST warm bias.

A further important validation of the 12 km RCM is to compare it to the equivalent simulation performed for Chapters 4 and 5. As discussed in section 2, for that stage the domain is slightly smaller and a different vegetation dataset is used. Furthermore, the present day simulation was initialised in 1980 and run for 30 years rather than being initialised in 1995 and run for 10 years. It is not obvious that any of these differences should affect significantly the mean climate. With this in mind, Figure A6.4 shows the seasonal mean rainfall differences between the Stage 3 and Stage 3b 12 km RCMs for the 10 year period common to both simulations. Note that the domain shown in this figure is larger than in other figures and extends west to the inner edge of the rim region of the Stage 3 domain. The differences in NDJ and FMAM (Figures A6.4(a) and (b)) are, as anticipated, small. However, the differences for JJA and SO (Figures A6.4(c) and (d)) are relatively large to the west of Singapore, with the Stage 3b model being wetter in the Strait of Malacca, over the sea to the west of Sumatra and over Singapore itself. These differences are likely due to the effects of natural variability, but given that they only occur in the south west monsoon season, it is also possible that there is a sensitivity of the rainfall over Singapore to the placement of the western boundary when the flow at that boundary has a westerly component.

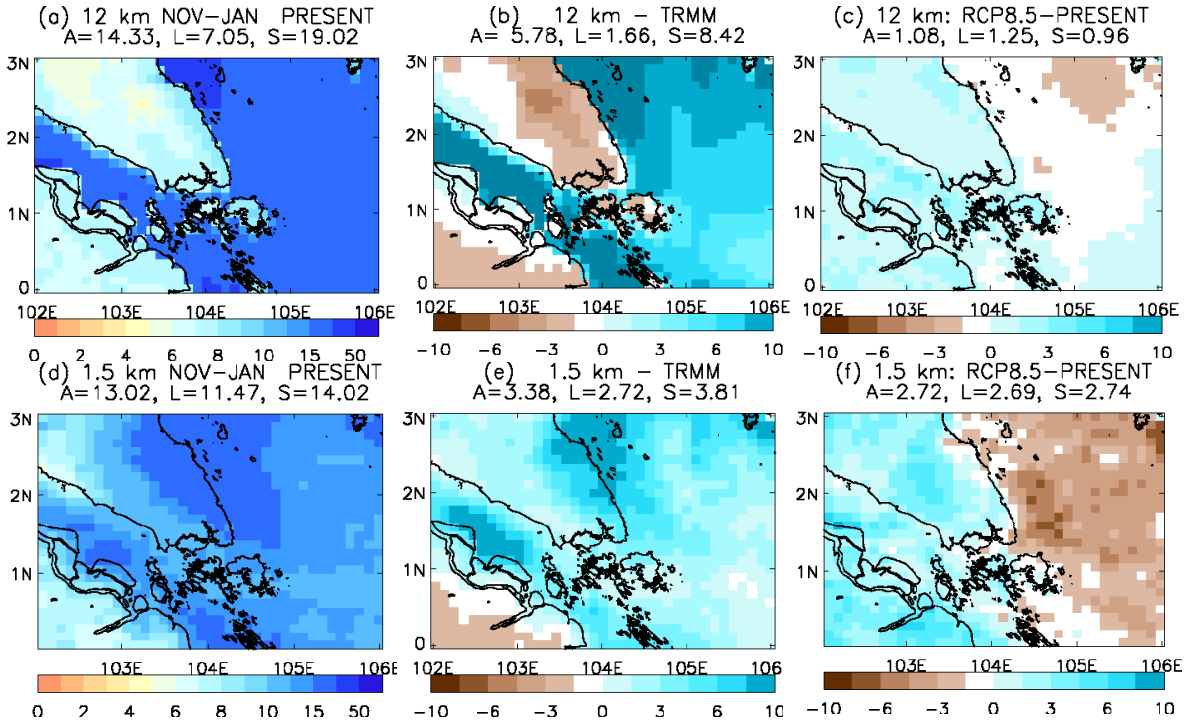

Figure 6.7: The NDJ mean rainfall in mm day^{-1} for the HadGEM2-ES driven simulations. (a) The 12 km RCM present day simulation, (b) the 12 km RCM present day bias relative to TRMM, and (c), the 12 km RCM climate change signal. (d) – (f) are as per (a) to (c), but for the 1.5 km RCM. The numbers in the title of each panel are labelled and calculated in the same way as described in figure 6.2.

Turning now to the climate change signal (Figs 6.7(c) and (f)), both models show an increase in rainfall over the western half of the domain (including Singapore) and a decrease over the eastern half of the domain (the South China Sea). The changes are generally larger for the 1.5 km RCM, although for Singapore itself the increase is

approximately the same in both models. Figure A6.3 shows that the same signals over the whole domain and over Singapore itself are evident in both models for the other three seasons with, in each case, the domain wide changes being larger in the 1.5 km RCM.

One potentially important issue with the above analysis is that it is based on 10 year simulations, which again means that the climate change signal may be affected by natural variability. This issue is investigated in Figure 6.8, which shows the Stage-3b 12 km RCM climate change signal in the left column. The other three columns show the climate change signal for the Stage-3 12 km RCM, where the difference is calculated for each decade of the RCP8.5 simulation relative to the 30 year mean for the present day simulation. There are two points to note from this figure. First, the Stage 3b climate change signal for all four seasons sits within the limits of the Stage 3 decadal differences. Second, and perhaps more importantly, the Stage 3 results appear to be robust from decade to decade over land, but are not robust over the sea. In particular, the differences for decade two in NDJ (Figure 6.8(c)) and decade one in FMAM (Figure 6.8(e)) are opposite in sign to that for the other two decades of those seasons. In other words, the Stage 3b climate change signal over land is likely to be robust whilst that over the sea it is not.

Returning now to Figure 6.3, the annual cycle of monthly mean rainfall for the present day simulations is shown in Figure 6.3(b). The simulations show many of the features identified in section 3.1.1 for the ERA-interim driven simulations. However, both models produce much more rainfall in the September to November period, and the 1.5 km RCM additionally moves its ERA-interim July peak earlier to May and June. As with the seasonal mean climate changes discussed above, these changes are most likely a reflection of the SST biases in HadGEM2-ES.

For the future climate simulations (Figure 6.3(c)), the annual cycle in both RCMs has, for the most part, moved later by approximately one month. Arguably the most striking difference between the two RCMs is the much larger amplitude change in the annual cycle in the 1.5 km RCM simulation, with both peak wet periods being wetter and both intermediate (drier) seasons being drier than either the 12 km RCM or the present day 1.5 km RCM.

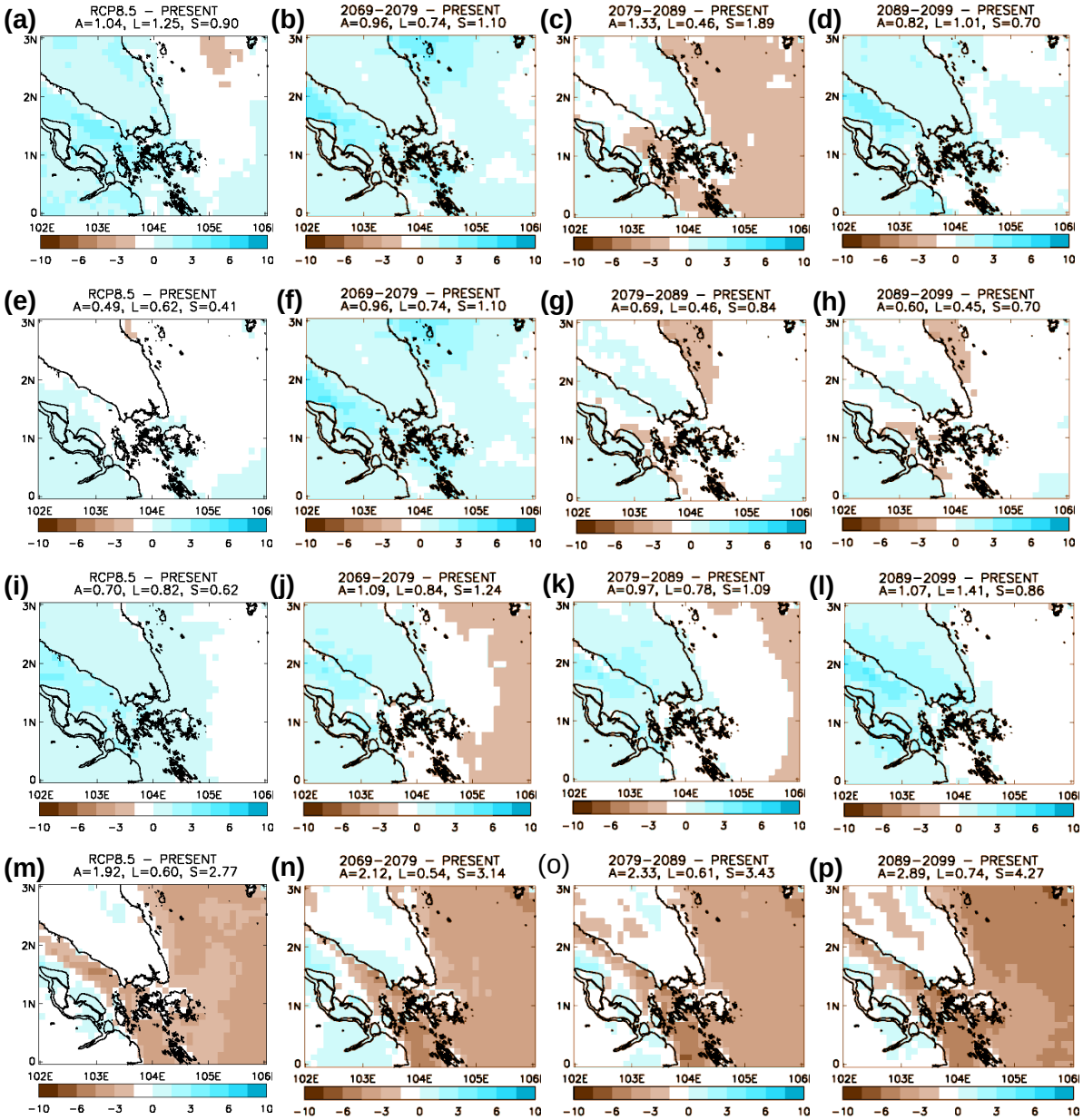

Figure 6.8. (a) The Stage 3b 12 km RCM mean rainfall climate change signal (2089-2099 minus 1995-2005) for NDJ. (b) The Stage 3 12km RCM mean rainfall climate change signal for the 2069-2079 decade relative to the present day (1975-2005) period. (c) as (b), but for the 2079-2089 decade and (d), as (b), but for the 2089-2099 decade. (e)-(h) As (a)-(d) but for FMAM, (i)-(l) as (a)-(d) for JJA and (m)-(p) as (a)-(d) but for Sep-Oct. Units are mm day^{-1}.

6.3.2.2 Extremes

In this section the projected change in extreme rainfall is assessed. Figure 6.9 shows the 95th percentile of the daily rainfall totals for the two RCMs. Both RCMs show increases in heavy rainfall over land in the future in NDJ (and in all seasons in fact, JJA being shown in Figure A6.5), with larger increases in the 1.5km RCM. In NDJ, the 12km RCM gives increases of 10-30% over land, whilst the 1.5km RCM shows increases of 30+%. Over sea, the 12km RCM suggests little change whilst the 1.5km RCM projects decreases of 10-30% over the South China Sea. Projected changes are very similar in JJA (Figure

A6.5) and Sept-Oct (not shown), except that the 1.5km RCM shows larger decreases of up to 50% over sea in these seasons and in Sept-Oct the 12km RCM shows smaller increases over land and decreases of 20-30% over sea. On considering a more extreme measure of precipitation (99th percentile of daily rainfall), projected changes are found to increase in relative terms but show a very similar spatial pattern. Changes in extremes on the hourly timescale (99th percentile of hourly rainfall; see Appendix to Chapter 6 figures A6.6-7) also mirror those on the daily timescale.

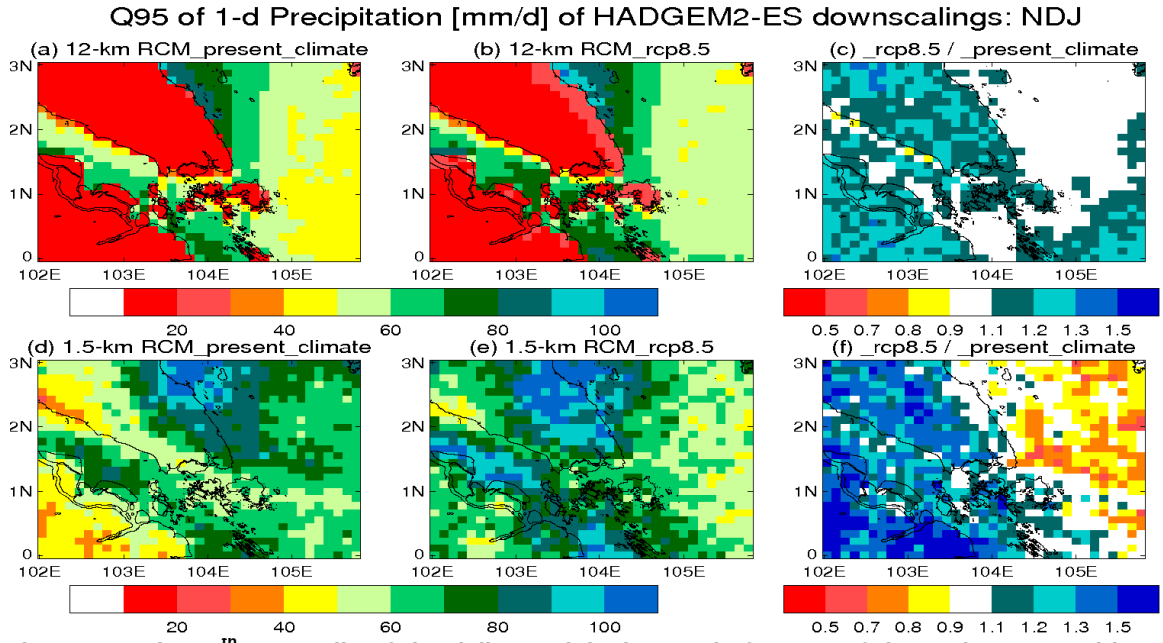

Figure 6.9: The 95^{tn} percentile of the daily precipitation totals for NDJ of the HadGEM2-ES driven simulations. (a) The 12 km RCM present day simulation, (b) the 12 km RCM RCP8.5 simulation and (c) the ratio of the future and present day climates. (d) - (f), as (a) –(c), but for the 1.5 km RCM.

6.3.2.3 Rainfall Intensity and Duration

Turning now to the intensity and duration of future rainfall, Figure 6.10 shows that there are two peaks in the 12 km RCM distribution over land, with a relatively high occurrence of short-duration low-intensity rain but also moderate intensity longer-duration rain. Over sea (Figure 6.11), the 12 km RCM shows a single peak in the distribution with short-duration low-intensity rain being most prevalent, and very little rain with peak intensities exceeding 10 mm hr^{-1}. By contrast, the 1.5 km RCM has much more rainfall at high intensity (>20 mm hr^{-1}) than the 12 km RCM, over both land and sea. Significant changes in the intensity-duration characteristics of rainfall are seen in the future. In both RCMs, and for both seasons examined here (see Figs A6.8 and A6.9 for the JJA plots), there is a shift to higher peak intensities in the future. In the case of the 1.5 km RCM, there is a significant increase in the relative occurrence of rain with intensities exceeding 20 mm hr^{-1}, over both land and sea. For the 12 km RCM, future increases are confined to much more moderate intensities, and in the case of sea points in NDJ there is less of a shift in intensity and more of a shift to shorter duration rain in future.

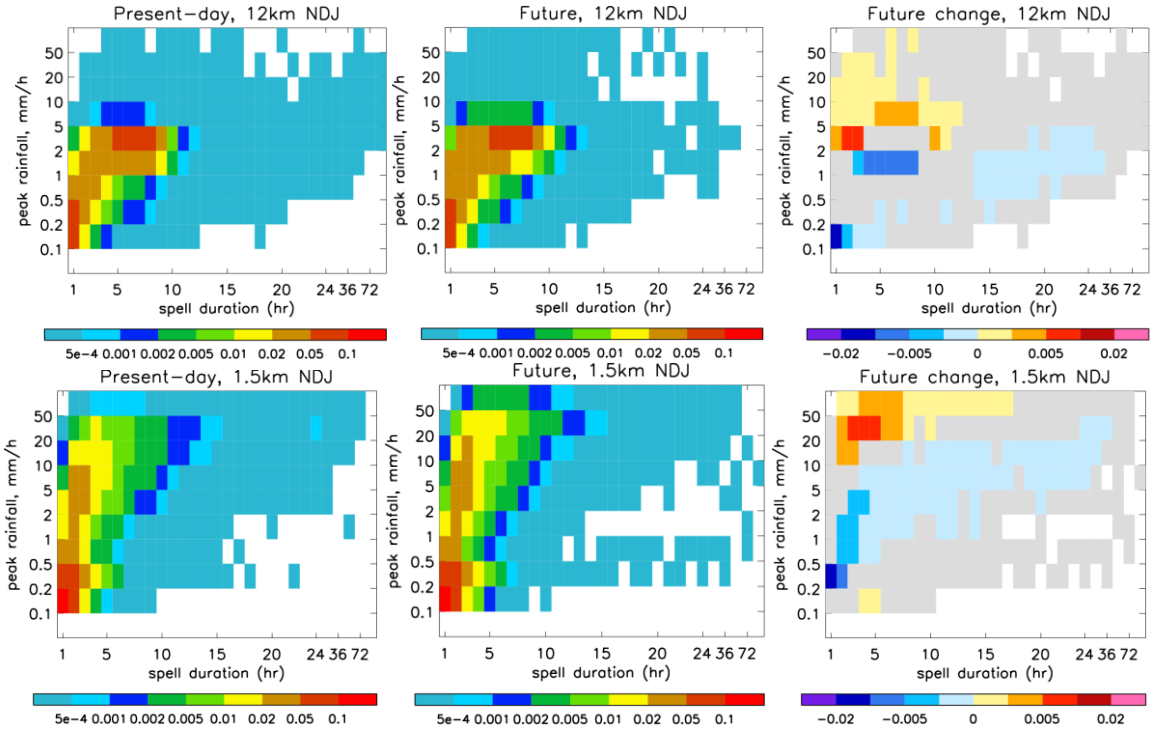

Figure 6.10: Joint probability distribution of wet spell duration versus peak intensity over land points for November-January. Shown are the present-day distribution (left), future distribution (middle) and future changes (right), for the 12km (top) and 1.5km (bottom) RCMs. Wet spells are defined as continuous periods when rain exceeds 0.1 mm/h. Changes that are not significant at the 1% level are masked in grey.

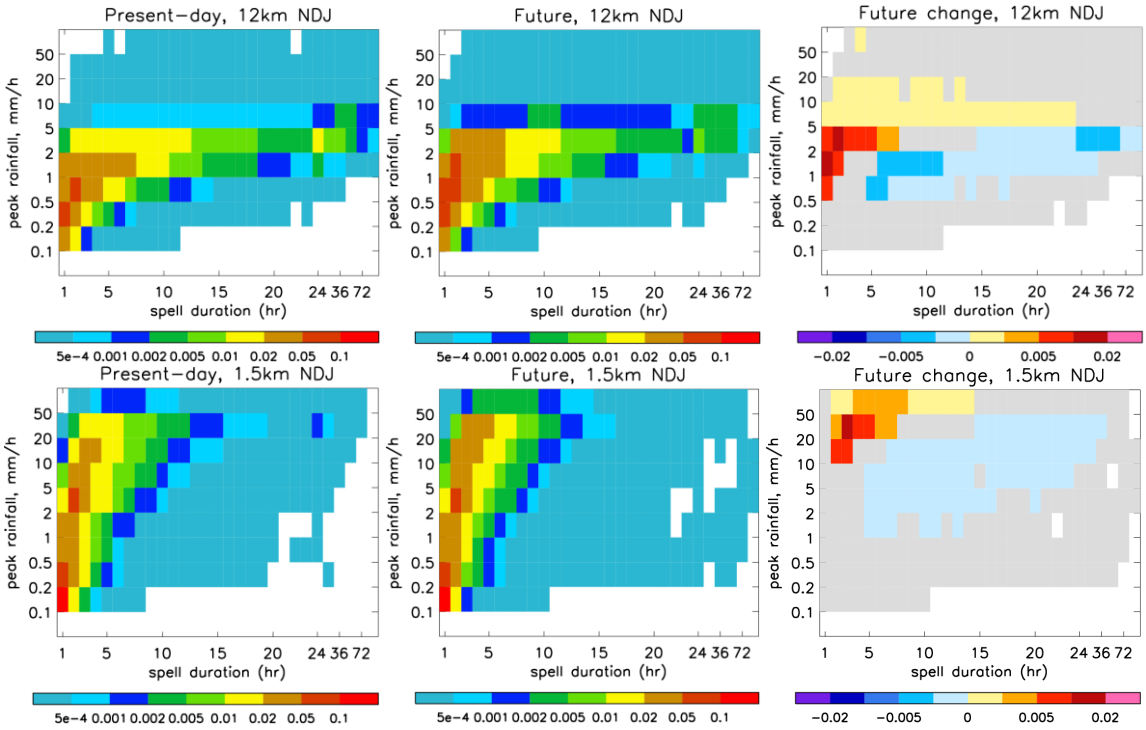

Figure 6.11: As Figure 6.10, but for sea points.

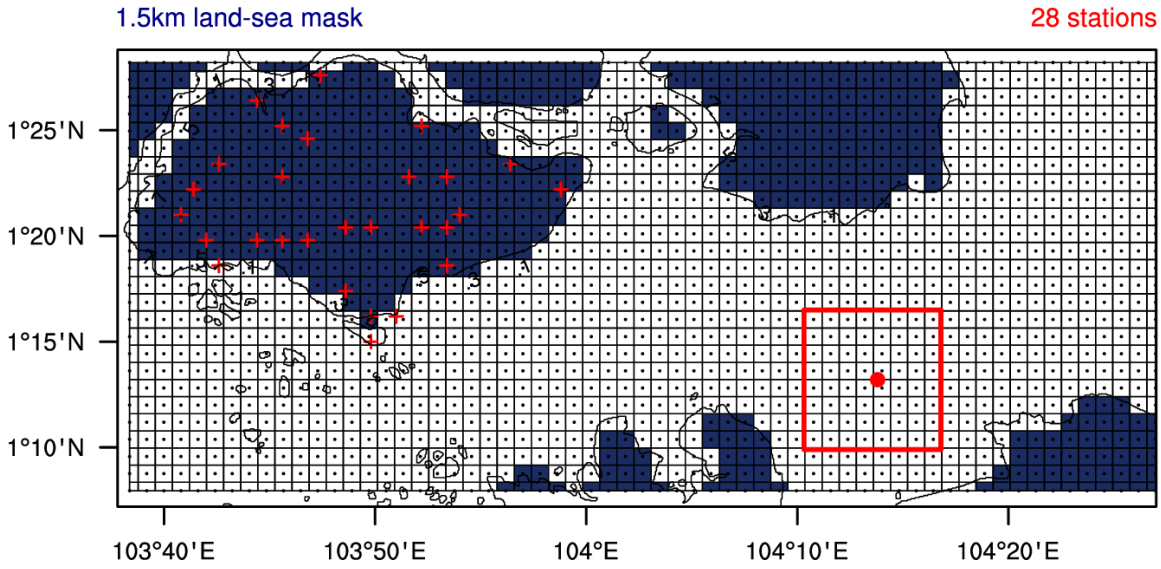

Figure 6.12: Land-sea mask in the 1.5 km RCM (dark blue), with grid boxes shown. The red crosses denote the locations of the 28 measuring stations across Singapore. The red box shows the location of the 12 km sea grid point used for quantile mapping.

6.3.3 Implications for Stage 3 downscaling assumptions.

The Stage 3 downscaled simulations have shown significant land-sea contrast of daily mean rainfall amounts when compared to station and TRMM data. However, cumulative distribution functions (CDFs) produced from a few modelled sea points compare very well, particularly in the extremes (see Figure 4.17, Chapter 4). The similarity between neighbouring sea-point CDFs and land observations at higher quantiles suggests that the distribution of daily mean rainfall over Singapore is not very different to that over adjoining seas, which is unsurprising given Singapore's maritime exposure.

Given the 12 km RCM shortcomings over land due to difficulties in capturing the diurnal cycle, and the resemblance of ocean CDFs with station observations at the extremes, it has been assumed that projected dynamically downscaled simulation values at a chosen nearby sea point can act as a reasonable proxy for Singapore's future rainfall on daily timescales after the necessary bias corrections (quantile mapping) are performed (see Climate Projections report). The selected sea point is shown in Figure 6.12, along with the locations of the 28 rain gauge stations. As a more realistic representation of rainfall is expected in the 1.5 km RCM by virtue of explicit convection and more accurate topography and coastlines, we use the high-resolution simulations to test the relationship between the two RCMs in supporting our assumption.

Figure 6.13 shows quantile distributions for both the historical (June 1995 – May 2005) and RCP 8.5 (June 2089 – May 2099) simulations. Station CDFs are plotted as black lines. The corresponding distributions for every 1.5 km grid point in which an observing station is located are plotted as orange lines, while the CDF obtained by averaging all 1.5 km daily data that lie within the 12 km ocean grid box is shown by the cyan line. The CDF obtained from the 12 km RCM point over Singapore is also plotted for comparison (magenta line). The key points from the figures are summarised below:

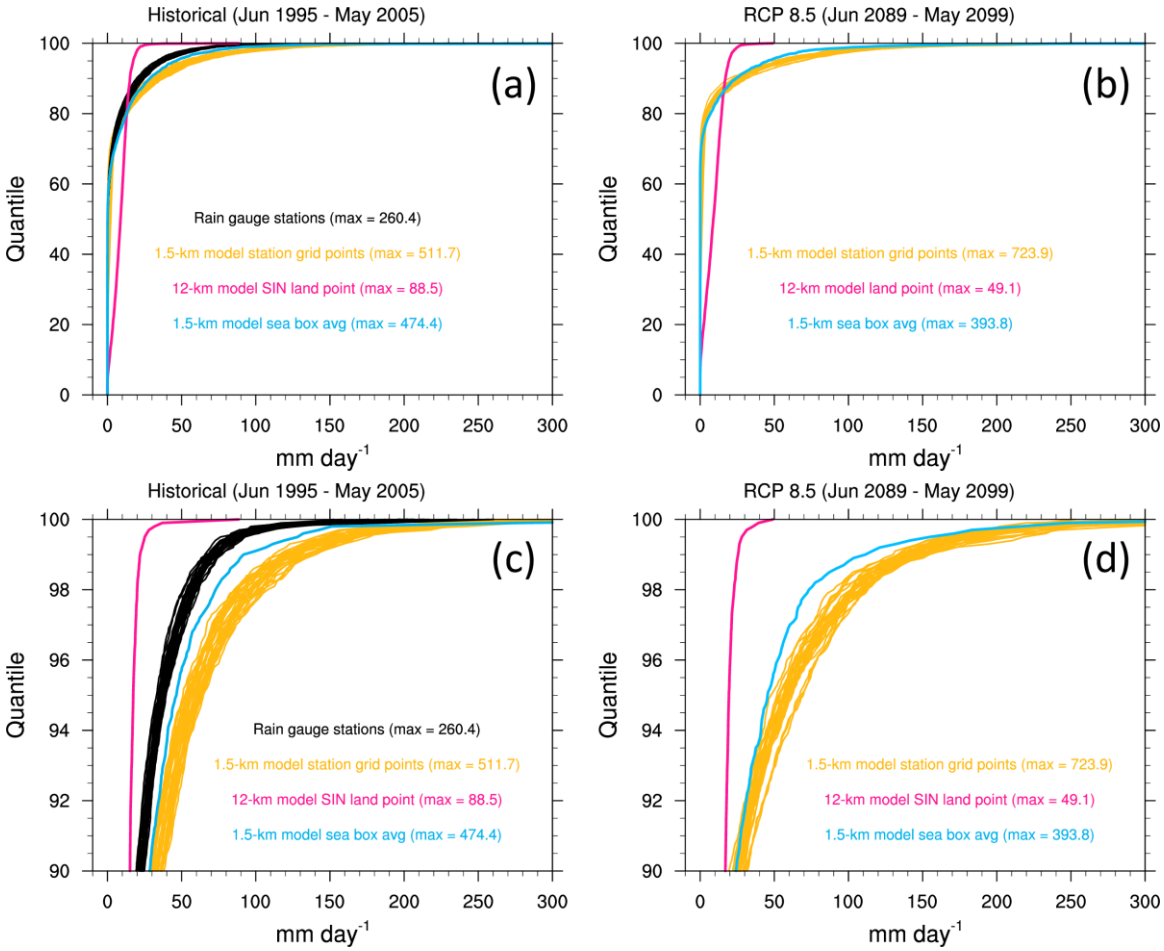

Figure 6.13: Quantiles (every 0.1% from 0.0 − 100.0%) of observed and modelled daily mean rainfall amounts (mm d^{-1}) for (a) historical and (b) RCP8.5 future climates. The black lines denote the cumulative distributions functions (CDFs) of the 28 station rain gauges. The orange lines show CDFs of only those Singapore grid points from the 1.5 km model that contain a station location within them (total of 28 points). The pink line denotes the CDF from the 12 km model for a centrally located Singapore land grid point. The cyan line depicts the CDF obtained by averaging all 1.5 km data within the chosen 12 km grid box over the sea. Maximum values for each set of CDFs are shown in parentheses. (c) and (d), as in (a) and (b), but for quantile 90 and above for visual emphasis.

Historical (June 1995 – May 2005)

1. The 1.5 km RCM over Singapore captures the station CDFs fairly well and better reproduces heavy rainfall events than the 12 km RCM, albeit with an overall wet bias above the 80th quantile and particularly at the upper 10 quantiles.

2. The 1.5 km RCM averaged within the selected 12 km sea box (blue line) also captures the station CDFs reasonably well, and matches better with station data than modelled 1.5 km land values (i.e., less bias) in the upper 10 quantiles (Figure 6.13(c) and (d)). This broadly justifies the use of a nearby sea point from the 12 km HadGEM2-ES (Stage 3) simulations to help project future daily rainfall statistics for Singapore after the necessary bias adjustments are performed (see Climate Projections report). However, it still overestimates most of the observed rainfall amounts above the 80th quantile.

3. The general shape and clustering of the 1.5 km land CDFs indicates that the RCM is able to generate a fairly realistic rainfall distribution over land that is comparable to historical rainfall distributions derived from station observations, despite the wet bias in the extremes.

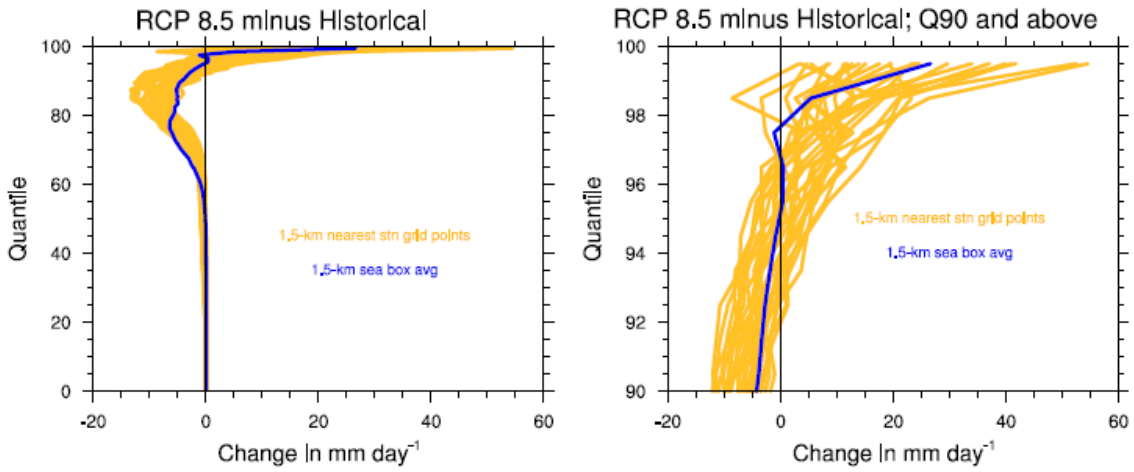

Figure 6.14: (a) Difference between the RCP 8.5 and historical daily rainfall amounts for every 0.05 quantile value up to the 99.5th quantile. (b) as in (a) but for the 90th quantile and above.

RCP 8.5 (June 2089 – May 2099)

1. The future 1.5 km RCM CDFs bears a similar resemblance to CDFs for the present climate below the 60th quantile (Figure 6.14 (a)) but show increases towards greater intensities above the 95th quantile (Figure 6.14 (b)). In broad terms, both land and sea end-of-century CDFs behave in a similar way in that they systematically shift towards larger values at the more extreme quantiles.

2. There is a tendency for more intense extremes over land than sea as more CDFs are shifted to the right above the 95th quantile (Q95) and a higher maximum value for the 99th quantile is modelled (Figure 6.14 (b)). This is consistent with the Q95 1-d rainfall spatial plots and the intensity-duration plots (Figures 6.9–11).

3. The intensity of Q95 extremes over the sea appear similar to the historical climate in the1.5 km model, with very little shift in the 12 km sea point future CDF; the shift towards heavier daily totals only occur above Q98 (Figure 6.14 (b)). This is perhaps partly explained by the location of the chosen point, which straddles the transition zone between two regions with different projected Q95 responses, i.e., stronger everywhere in areas west of 104°E and weaker or negligible in regions east of 104°E (c.f. Figure 6.9).

It is also prudent to realise that only one convective-scale model realisation was used for RCP 8.5 in this case. Hence, the behaviour seen in the future CDFs may not necessarily be significant in the context of climate change. Any changes seen can be interpreted to lie within the bounds of inter-annual variability. Further analysis is required to understand the reasons for the different end-of-century response between the 1.5 km and the 12 km models.

The sensitivity to the choice of sea point around Singapore was also evaluated (though not shown here). Essentially, there is very little difference in the characteristics and behaviour of any 12 km sea point east of Singapore between 104°E-104.5°E, in both present and future climates. Any nearby eastern sea point captures the station data very well and lies within the envelope of station and 1.5 km RCM CDF curves over land. However, CDFs from sea points to the west of Singapore between 103.5°E-103.75°E tend to overestimate station values at the upper quantiles with biases similar to those from the 1.5 km RCM land points over Singapore. The selection of the original sea point for quantile mapping is therefore appropriate.

6.4 Summary

In this report we have assessed the ability of a convective-scale dynamically downscaled model to simulate the local climate of Singapore. A 1.5 km resolution regional climate model (RCM) is nested within one of the 12 km RCMs used in Stage 3 of the V2 project. The ability of the 1.5 km RCM to simulate the present day climate is assessed through an analysis of an ERA-interim driven simulation, whilst the projected climate change from this RCM is assessed in present day and RCP 8.5 simulations driven by HadGEM2-ES. The three simulations are all ten years in length (their duration is limited by the computational expense of the convective-scale RCM) and the results presented focus on the realism of the simulated rainfall, in terms of the mean climate and the ability of the RCMs to simulate extremes.

The key findings from the present day climate assessment are as follows: -

- The simulation of daily and sub-daily rainfall features are greatly improved in the 1.5 km RCM, consistent with results for the UK (Kendon et al., 2012). Using TRMM to validate the models, the diurnal cycle of rainfall over land is found to be improved in the 1.5 km RCM compared to that in the 12km RCM, with the peak in the rainfall occurring later in the day and with the amplitude reduced by approximately a factor of two. Furthermore, the simulation over land of daily and sub-daily extremes is also much more realistic in the 1.5 km RCM, with the extreme rainfall (95^{th} and 99^{th} percentiles) typically two to three times heavier than in the 12 km RCM.
- The mean rainfall distribution in the 1.5 km RCM is superior to that in the 12 km RCM in some respects and worse in others. Improvements are seen in the land/sea distribution with much reduced gradients across coasts. The ability of rain-bearing systems to propagate in-land leads to a much-improved simulation of the north-east monsoon over Malaysia. Furthermore, the timing of the peak in the north-east monsoon rainfall is improved in the 1.5 km RCM, with it occurring in November (one month early) rather than September. However, the 1.5 km RCM driven by ERA-interim is 15-20% drier in the annual mean than both the 12 km RCM and TRMM.
- Most of the mean rainfall differences between the 1.5 km and 12 km RCMs are evident when the intermediate 4.5 km RCM is compared to the 12 km RCM. The differences between the two convection permitting models (the 1.5 km and 4.5 km RCMs) are much smaller. The largest change in the rainfall distribution therefore occurs between the models where the convection is parametrized in one and represented explicitly in the other. The spin-up of explicit convection from the parametrized convection flow fields specified at the lateral boundaries of the 4.5 km RCM leads to time mean differences which can extend more than 200

km into the domain and hence suggest that the 4.5 km RCM (and 1.5 km RCM) might be sensitive to the 4.5 km RCM domain size.

The key findings from assessing the future projections for 2089-2099 under RCP8.5 (referred to as end-of-century projections in what follows) are as follows: -

- End-of-century projections for the seasonal mean rainfall show a modest increase over land (including Singapore), and a decrease over the sea. This conclusion applies equally to both RCMs. Projections for the annual cycle of monthly mean rainfall over Singapore itself show a much larger amplitude change in the 1.5 km RCM, with both wet seasons being wetter and both intermediate seasons being drier than either the 12 km RCM or the present day 1.5 km RCM. However, as discussed in the bullet point that follows, these results should be treated with caution since they will be affected by natural variability.
- End-of-century projections based on the longer Stage-3 12 km RCM simulations for the seasonal mean rainfall show that over the South China Sea decadal variability dominates the overall long term trend and hence the sign of the rainfall change over the sea varies between decades. Over land the increased rainfall signal appears more robust. This emphasises that caution must be taken in interpreting the 12 km and 1.5 km end-of-century projections since they will be affected by natural variability. This is an inevitable consequence of the analysis being restricted to a single 10-year-long convective-scale model realisation of the climate of Singapore.
- End-of-century projections for extreme daily rainfall show an increase over land in all seasons, with the increase being larger for the 1.5 km RCM. Over the ocean, the 1.5 km RCM projection reveals an emerging decrease in extreme precipitation that is not present in the 12 km RCM.
- End-of-century projections for hourly rainfall intensity and duration show a significant increase in the occurrence of rainfall events (intensities exceeding 20 mm hr^{-1}) over both land and sea in the 1.5 km RCM. In contrast for the 12 km RCM, the increased occurrence of rainfall is limited to rainfall intensities less than 10 mm hr^{-1}.
- The 1.5 km simulations support the assumptions that were necessary to bias correct precipitation outputs from the set of nine 12 km RCM climate projections over Singapore. In the 1.5 km RCM, the rainfall distributions are similar over Singapore land points and the nearby ocean point that was used for bias correction. Also the mean signal for future change over Singapore is not altered in the 1.5 km RCM; however there is a large spread and more spatial variability in the high resolution simulations.

6.5 Recommendations and Limitations

As already discussed in the main body of the text, the main limitation of this study is that the results and associated conclusions will be affected by natural variability, which is an inevitable result of the simulations being restricted to ten years in length. Furthermore, it is important to remember that only a single convective-scale RCM has been used in this study, and that the results will inevitably be sensitive to the choice of the RCM.

This report has focussed entirely on the simulated rainfall, its sensitivity to resolution and its projected end-of-century change. Other fields such as near-surface winds will also be

very different in the 1.5 km RCM since it represents explicitly the three-dimensional circulations associated with deep convection, and hence it includes an explicit representation of wind gusts. It is recommended that these winds be compared to the 12 km RCM winds and that the analysis performed is as detailed as has been the case for the rainfall in this study.

Finally, results from the 4.5 km RCM simulation have not been analysed or discussed in detail in this report because NWP investigations using convection permitting versions of the Unified Model over Singapore (in the SINGV project) and elsewhere in the tropics indicate that the 1.5 km model performance is much superior to that at 4.5 km resolution. However, it is not obvious that the superiority of the 1.5 km RCM over the 4.5 km RCM will be so apparent for climate simulations, since it is possible that the NWP result is dominated by the response of the respective models to the initial conditions. Moreover, a brief inspection of some of the 4.5 km model fields suggests that many of the changes described in this study regarding the improved performance of the 1.5 km RCM are seen in the 4.5 km RCM. This suggests that the key change when moving from the 12 km parametrized convection configuration to the 1.5 km convection permitting configuration is the change in the representation of convection rather than the refinement of the mesh size. It is therefore recommended that a detailed investigation of the 4.5 km model is performed since, potentially, it could provide climate change projections of comparable quality to those deduced from the 1.5 km RCM in this study, but at one third the computational cost of this study.

Acknowledgements

We would like to thank Simon Wilson for the technical assistance in setting up these simulations on the ECMWF Cray. We would also like to thank Simon Tucker and Grace Redmond for generating the SST and ozone ancillary files for the simulations.

References

Boutle, I. A., Eyre, J. E. J. and Lock, A. P. (2014). Seamless Stratocumulus Simulation across the Turbulent Gray Zone. Mon. Weather Rev., 142, 1655-1668.

Kendon, E. J., Roberts, N.M., Senior, C. A. and Roberts, M. J., (2012). Realism of rainfall in a very high resolution regional climate model. J Climate, 25, 5791-5806.

Kendon E.J., Roberts, N.M., Fowler, H.J., Roberts, M.J., Chan, S.C.and Fowler, C.A. (2014). Heavier summer downpours with climate change revealed by weather forecast resolution model. Nature Climate Change, 4, 570-576 doi: 10.1038/NCLIMATE2258.

Wilkinson, J. M. and Bornemann, J. (2014) A lightning forecast for the London 2012 Olympics opening ceremony. Weather 69:1, 16-19.

Wood, N. Staniforth, A. White, A., Allen, A. Diamantakisa, M., Gross, M., Melvin. T., Smith, C. Vosper, S. Zerroukat, M. and Thuburn, J. (2014) An inherently mass-conserving semi-implicit semi-Lagrangian discretisation of the deep-atmosphere global nonhydrostatic equations. Quart. J. Roy. Meteorol. Soc., 140, 1505-1520 DOI: 10.1002/qj.2235